Article

Novel Detection Method for Consecutive DC Commutation Failure Based on Daubechies Wavelet with 2nd-Order Vanishing Moments

Tao Lin [1], Ziyu Guo [1,*], Liyong Wang [2], Rusi Chen [1] and Ruyu Bi [1]

[1] School of Electrical Engineering, Wuhan University, Wuhan 430072, China; tlin@whu.edu.cn (T.L.); 2014102070014@whu.edu.cn (R.C.); biruyu@sina.com (R.B.)
[2] State Grid Beijing Electric Power Company, Beijing 100031, China; 13810007912@163.com
* Correspondence: 15071113736@163.com; Tel.: +86-150-7111-3736

Abstract: Accurate detection and effective control strategy of commutation failure (CF) of high voltage direct current (HVDC) are of great significance for keeping the safe and stable operations of the hybrid power grid. At first, a novel detection method for consecutive CF is proposed. Concretely, the 2nd and higher orders' derivative values of direct current are summarized as the core to judge CF by analyzing the physical characteristics of the direct current waveform of the converter station in CF. Then, the Daubechies wavelet coefficient that can represent the 2nd and higher order derivative values of direct current is derived. Once the wavelet coefficients of the sampling points are detected to exceed the threshold, the occurrence of CF is confirmed. Furthermore, by instantly increasing advanced firing angle β in the inverter side, an additional emergency control strategy to prevent subsequent CF is proposed. Eventually, with simulations of the benchmark model, the effectiveness and superiorities of the proposed detection method and additional control strategy in accuracy and rapidity are verified.

Keywords: HVDC; consecutive commutation failure; Daubechies wavelet; 2nd-order vanishing moments; wavelet coefficient

1. Introduction

Commutation failure (CF) is a common threat to high voltage direct current (HVDC). Due to the application of thyristor, strong reactive support from an AC system is needed for guaranteeing the normal operation of HVDC. Therefore, the drop of converter bus voltage caused by AC fault is the main reason for commutation failure of converter station, especially in the inverter side [1–4]. CF increases the direct current, resulting in converter transformer DC bias and inverter system over-voltage. An emergency controller based on a quick CF detection method can effectively reduce the duration of CF and promote extinguishing angle recovery, which means better economy and faster voltage recovery [5–8].

More importantly, to protect the valves from high current during CF, the valve lockout controller will lock them after detection of CF. As most AC faults are temporary and the restart of HVDC takes time and results in power imbalance, it is conservative to lock the valves after the occurrence of single CF [9]. In contrast, it is more sensible to lock the valves after the occurrence of consecutive CF, namely, there exist continuously two or multiple CFs. Therefore, the accurate detection of CF, especially detection of consecutive CF, is of significant importance for safe operation of power systems [10].

The issue of the detection of CF has been gained comprehensive attention. A series of literature was proposed. Specifically, the methods of these papers can be divided into two categories:

(1)	The methods based on measurement. By measuring the time interval between the end of each valve current and the next commutation voltage zero crossing point to obtain the extinguishing angle γ, occurrence of CF is judged by comparing γ and its extreme value [11–15]. The method based on measurement is put into use in a Tian-Guang HVDC system in Guangzhou, China. The limitation lies in the fact that an extinguishing angle exceeding the threshold does not necessarily cause CF. In addition, methods based on measurement give out the result at the end of each commutation process, which causes delay. In addition, the extreme value of extinguishing angle is usually considered to be $7°$–$10°$ in different studies [16–18]. The absence of a unified indicator will cause misunderstanding.

(2)	The methods based on prediction. These methods use bus voltage or other electrical quantities during the AC fault to determine whether CF occurs [19]. Concretely, in [20,21], the voltage and current are subjected to an abc–$\alpha\beta$ transformation and the resulting zero sequence components are used to determine whether CF occurs. A similar method is put into use in the San-Guang HVDC system in Guangzhou, China [22,23]. Ref. [24] presents a criterion of CF by comparing direct and alternative currents in fault. A fuzzy controller to minimize CF is later established. The commutation failure immunity index (CFII) has been proposed in recent years to quantify the immunity of a converter to CFs by comparing the grounding impedance with its critical value [13]. However, the harmonics and dynamic behavior of controllers should be further considered to improve the accuracy. In addition, neither the methods based on measurement nor the methods based on prediction can detect CF that is caused by trigger pulse losing.

In recent years, detection methods of CF via analyzing the real-time waveform were proposed and obtained favorable results. Ref. [25] diagnoses CF in HVDC systems based on wavelet transforms of direct voltage. Daubechies-4 (db4) wavelet is served as the wavelet basis function for the detection and classification of faults. The resolution level is up to 6, thus increasing the computation. In addition, its detection performances for continuous faults need further improvements. Ref. [26] proposed a CF diagnosis method based on the singular value decomposition and support vector machines. However, its accuracy in the time domain needs to be improved. The CF time cannot be exactly determined. Ref. [17] extracts fault features of direct current in types of faults by wavelet energy spectrum. Grey comprehensive correlation degree analysis method is then used to distinguish them. The flaw is that differences between CF and non-CF faults need further study.

The above methods all aim at single CF occurrence and are weak at judging the accurate CF time. Few studies focus on detection of consecutive CF and their exact time. In Ref. [27], mathematical morphology is introduced to calculate the gradient of direct current. The point whose gradient exceeds the threshold is taken as the CF point. The principle is simple and fast. However, for the work of the voltage dependent current order limiter (VDCOL), the gradient of direct current may exceed in some non-commutation failure point, which may result in misjudgments. The precise consecutive CF detection method is worthy of in-depth study to provide a reasonable criterion for the operation of the emergency controllers, such as the valve lockout controller.

In this paper, a novel detection method for consecutive CF is proposed. By analyzing the physical characteristics of the direct current waveform in CF, the 2nd and higher orders derivative values of direct current are summarized as the core to judge CF. Then, the Daubechies wavelet with 2nd-order vanishing moments, which can represent the 2nd and higher orders derivative values of direct current, is derived. Once the wavelet coefficients of the sampling points are detected to exceed the threshold, the occurrence of CF is confirmed. Furthermore, by instantly increasing advanced firing angle β in the inverter side, an additional emergency control strategy to prevent subsequent CF is proposed.

2. The Principle of CF Detection by Current Waveform Singularity

As the basis, the characteristic of directs current in CF is analyzed to guide the detection of CF.

2.1. Characteristics of Direct Current in CF

In this paper, the International Council on Large Electric systems (CIGRE) benchmark [28] model shown in Figure 1 is used to carry out analyses. The rectifier control system is with constant current control, and the inverter side is with constant extinguishing angle (CEA) control. R, L, C stand for the resistance, reactance and capacitance of DC line, respectively. The valve position of the inverter is illustrated in Figure 2, where I_d stands for the direct current; L_b stands for the transformer leakage reactance. V_1 to V_6 stand for the valve No. 1 to No. 6. All faults are set to occur at the commutation bus at 1.0 s.
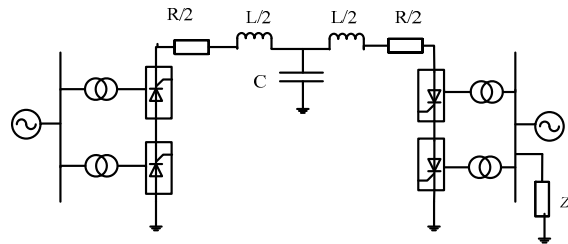

Figure 1. International Council on Large Electric systems (CIGRE)-benchmark model.
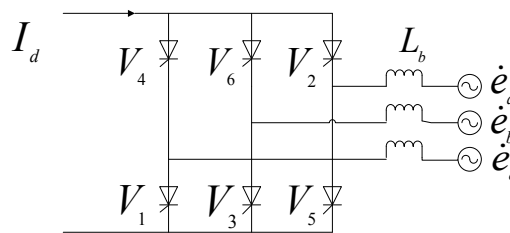

Figure 2. Valve position of the inverter.

A three-phase grounding fault with Zf = 100 Ω is first presented. The waveforms of direct current I_d, current of converter valve No. 2 I_2, and current of converter valve No. 5 I_5 are shown in Figure 3.
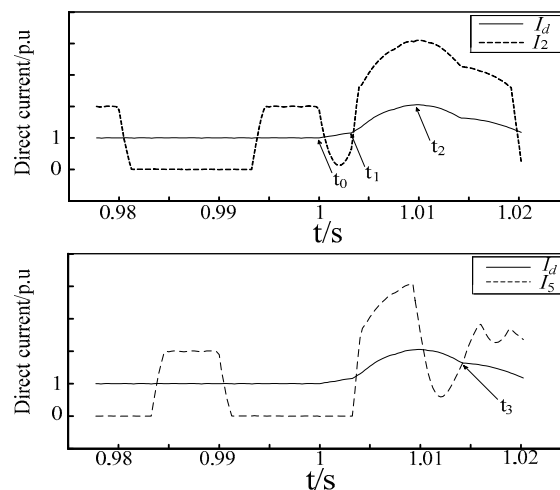

Figure 3. Direct current and Nos. 2 and 5 valve current in three-phase grounding fault.

It should be noted that, in Figure 2, the ordinate represents the direct current value. The valve current wave only represents its waveform. The direct current and valve current are shown in the same plot to show the relative relationship between them during the CF process. The other figures in this article are the same as this example.

When CF occurs, direct current jumps due to the short circuit of converter. It often reaches twice the value of the steady-state value and then declines with the work of VDCOL. The process consists of three stages:

(1) t_0–t_1 stage, the AC fault has just occurred and the inverter side AC voltage is reduced, resulting in the drop of DC voltage in the inverter. The direct current began to rise, but, by the existence of a flat wave reactor, the rise is small.

(2) t_1–t_2 stage. Before time t_1, valve No. 4 is closed prematurely due to insufficient phase voltage. The direct current flows back to valve No. 2, who should shut down before t_1. With the normal conduction of valve No. 5, 2-5 bridge forms a DC side short circuit and the direct current has a significant growth at t_1. The first CF occurs.

Due to the role of the VDCOL, the direct current growth slows down and reaches the maximum at time t_2 (hereinafter referred to as the controller point), and then begins to reduce.

(3) t_2–t_3 stage. Due to AC voltage reduction and the high level direct current, valve No. 1 is closed prematurely and the current flows back to valve No. 5. With normal conduction of valve No. 2, 2-5 bridge once again forms a DC short circuit and direct current reduction rate slows down at t_3. The 2rd CF occurs.

2.2. Summary of DC Current Variation in the CF Process

From the analysis above, the following conclusions of the direct current can be summarized.

(1) The singularity of direct current at t_1 and t_3 could represent the occurrence of DC short circuit, which is the inevitable result of CF. Through the detection of these singular points, the occurrence of CF can be identified.

(2) When the system is in normal operation, there are ripples in the direct current wave form and the second and higher derivative of the current waveform are nonzero in these points. However, when CF occurs, direct current mutations are prominent in addition to the corresponding second and higher derivatives.

By observing the second and higher derivatives of these singular points, the moment of CF can be detected precisely. A wavelet with moment selection characteristics could well satisfy the need for detection of excessive derivative values. The first derivative of the waveform must be shielded so that the wavelet coefficients are not affected by the current increase during the fault. A wavelet function with 3rd-order vanishing moments is obviously excessive because the second-order derivative plays an important role in the detection of singularity in CF. In this paper, the Daubechies wavelet with 2nd-order vanishing moments is utilized to analyze the direct current. When wavelet coefficients exceed the threshold, CF is determined to occur.

3. Principle of Daubechies Wavelet with 2nd-Order Vanishing Moments Detection Method

According to the above analysis, this chapter is based on Daubechies wavelet with 2nd-ordervanishing moments to obtain 2nd and higher order information of DC waveform.

Daubechies wavelet has the shortest support set for any given vanishing moment n, and the detection of the waveform singularity is accurate in the time domain [29]. Daubechies wavelet has no specific analytic expression, and its scale function ϕ and wavelet function ψ are iterated by the following formula [30]:

$$\phi_0(x) = \begin{cases} 1 & 0 \leq x < 1 \\ 0 & \text{else} \end{cases}$$
$$\phi_n(x) = \sum_{k=0}^{3} P_k \phi_{n-1}(2x - k) \tag{1}$$
$$\psi_n(x) = \sum_{k=0}^{3} (-1)^k P_{3-k} \phi_n(2x - k).$$

With different P_k, the wavelet function has a different vanishing moment. The wavelet vanishing moment is defined as: for a distribution ψ, the smallest integer n that satisfies Equation (2) is the vanishing moment of the ψ:

$$\int_{-\infty}^{\infty} x^n \psi(x)dx \neq 0. \tag{2}$$

Dr. Daubechies first obtained the wavelet function with the 2nd-order vanishing moment. Its coefficient P_k are as Equation (3), and its corresponding wavelet waveform is shown in Figure 4:

$$P_0 = \frac{1+\sqrt{3}}{4}, P_1 = \frac{3+\sqrt{3}}{4}, P_2 = \frac{3-\sqrt{3}}{4}, P_3 = \frac{1-\sqrt{3}}{4}. \tag{3}$$

Figure 4. Waveform of Daubechies wavelet with 2nd-order vanishing moment.

The wavelet coefficient b_k^j by wavelet analysis of a particular sequence $f(x)$ are given as follows:

$$
\begin{aligned}
b_k^j &= \int_{-\infty}^{\infty} f(x)2^j \psi(2^j x - k)dx \\
&= \int_{-2^{-j}}^{2^{1-j}} f(x + 2^{-j}k)2^j \psi(2^j x)dx,
\end{aligned} \tag{4}
$$

where k represents the amount of data translation, and j represents the resolution. For the second line of Equation (4), the 2nd-order Taylor expansion is as Equation (5):

$$f(x + 2^{-j}k) \approx f(2^{-j}k) + xf'(2^{-j}k) + \frac{1}{2}x^2 f''(2^{-j}k) + O(2^{-j}k), \tag{5}$$

where $O(2^{-j}k)$ indicates its high order term. Then, Equation (4) can be expressed as:

$$
\begin{aligned}
b_k^j &= \int_{-2^{-j}}^{2^{1-j}} f(x + 2^{-j}k)2^j \psi(2^j x)dx \\
&= \int_{-2^{-j}}^{2^{1-j}} [f(2^{-j}k) + xf'(2^{-j}k) + \frac{1}{2}x^2 f''(2^{-j}k) + O(2^{-j}k)]2^j \psi(2^j x)dx.
\end{aligned} \tag{6}
$$

Since $\psi(x)$ has a 2nd-order vanishing moment, Equation (7) is established:

$$\int_{-2^{-j}}^{2^{1-j}} f(2^{-j}k)\ \psi(2^j x)dx = \int_{-2^{-j}}^{2^{1-j}} xf'(2^{-j}k)\ \psi(2^j x)dx = 0. \tag{7}$$

Substituting Equation (7) into Equation (4), there is:

$$b_k^j = \int_{-2^{-j}}^{2^{1-j}} [\frac{1}{2}x^2 f''(2^{-j}k)\psi(2^j x) + O(2^{-j}k)]dx. \tag{8}$$

By Equation (8), the wavelet coefficients are only related to the 2nd and higher order derivative of the sequence $f(x)$ at data point k. The 2nd-order Daubechies analysis can be used to obtain the

information of the 2nd and higher order derivative at each sample point, so as to determine whether CF occurs.

The value of the wavelet coefficient is calculated by Formula (6). It can be seen from the formula that the size of the wavelet coefficient is determined by the window of the wavelet function and the sampling frequency of the original data. In this article, the raw data comes from the simulation of the EMTDC/PSCAD (V4.2.1, Manitoba HVDC Research Center, Winnipeg, MB, Canada) software at a sampling frequency of 4000 Hz. The window of the wavelet function is 769. Under this condition, the maximum value of the wavelet coefficient t in non-CF fault is 0.1391. Considering a certain amount of reservation, the threshold value is empirically set to 0.15.

4. Additional Emergency Control for CF

When the reduction of extinguishing angle γ is detected, the order of advanced firing angle β in the inverter side will be increased by the CEA controller, which is helpful for HVDC to mitigate the CF and to improve the system recovery performances [20]. However, there exists a milliseconds delay to measure the extinguishing angle; thus, the extinguishing angle reduction is not sensitive enough to be obtained, which may lead to subsequent occurrence of CF.

In this section, based on the accuracy and sensitivity of the proposed detection method, an additional emergency control for CF (AECCF) is proposed to prevent subsequent occurrence of CF. As shown in Figure 5, concrete steps of AECCF are as follows:

- Step (1) Monitor wavelet coefficient of direct current. Once the wavelet coefficients exceed the threshold, CF is determined to occur.
- Step (2) Set the β order in the inverter side to the emergency valve β_e. $\beta_e = $ M × β order 1.
- Step (3) A timer is added to set the duration of this emergency control. In this paper, the duration is set as 0.01 s, which is sufficient for automatic control device to remove the fault.
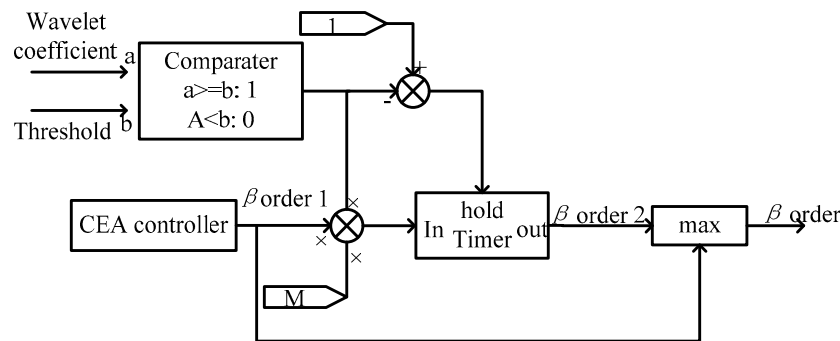

Figure 5. Control diagram of the additional emergency control for commutation failure (CF).

The emergency valve β_e is based on the following formula:

$$\beta_e = \arccos(\cos(\gamma_0) - \frac{2X_B I_d}{\sqrt{6}U_1}). \tag{9}$$

γ_0 represents the steady-state value of extinguishing angle γ, X_B stands for the commutation reactance, and U_1 stands for the AC voltage when γ is at the critical value $\gamma_{\min}$ [16]:

$$U_1 = \frac{2X_B I_d}{\sqrt{6}(\cos(\gamma_{\min}) - \cos(\beta_0))}, \tag{10}$$

where β_0 stands for the steady-state value of β.

The proposed AECCF strategy takes effect only when CF is determined to occur. By this way, it can reduce the chances of subsequent CF while not affecting the economic operation of the DC system.

The proposed CF detection method is based on the direct current waveform, which is available for the converter station. The whole process of the proposed CF detection method and AECCF are closely related. Therefore, the fast response of AECCF is guaranteed by the rapidity of the proposed CF detection method.

5. Simulation Analysis

In order to verify the accuracy and universality of the proposed method and additional emergency control, the following types of faults are validated, respectively. The direct current sampling dates are obtained from the EMTDC/PSCAD simulation and the sampling interval is 250 μs. The 2nd-order vanishing moment Daubechies wavelet function is used to process the direct current with eight iterations. The wavelet data length is 769. Between adjacent direct current sampling points, linear interpolation is used to add 769 data. At this sampling frequency and wavelet data length, this paper concludes that 0.15 is a reasonable threshold for wavelet coefficients to determine whether CF occurs.

5.1. Verifications of the Proposed Detection Method

5.1.1. Three-Phase Grounding Fault Detection Results

A three-phase grounding fault example is shown in Figure 3, with $Zf = 100\ \Omega$. The corresponding wavelet coefficients are shown in Figure 6. The detection results are illustrated in Table 1.
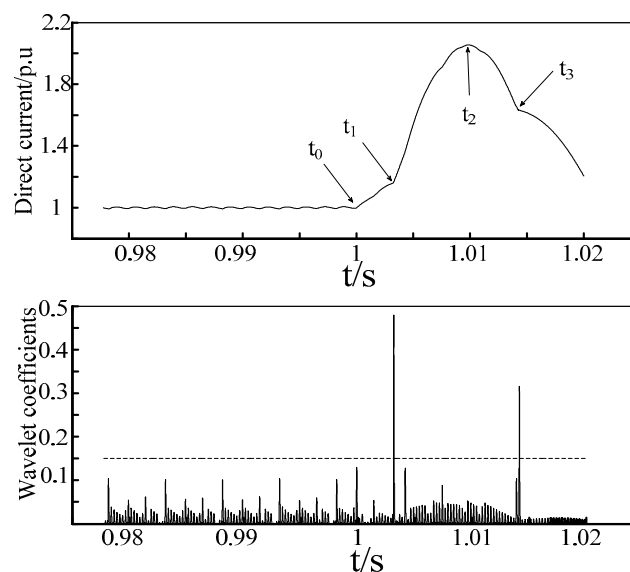

Figure 6. Direct current wavelet coefficients of three-phase grounding fault.

Table 1. Simulation and detection result of commutation failure (CF) moments in three-phase fault.

Comparasion	1st CF (t_1)	2nd CF (t_3)	Controller Point
Simulation	1.003 s	1.014 s	1.009 s
Proposed method	1.003 s	1.014 s	Not detected

In this example, CF moments $t_1 = 1.003$ s, $t_3 = 1.014$ s are detected for the prominent wavelet coefficients, which are 0.3589, 0.2139, respectively. The fault time $t_0 = 1.000$ s and the current inflection point (by VDCOL) $t_2 = 1.011$ are not detected.

5.1.2. Single-Phase Fault Detection Results

- • (a) Detection results for serious single-phase fault

For the HVDC benchmark, set the fault as C phase grounding fault in the inverter with Zf = 70 Ω. The current waveform in this case is analyzed and the CF points are detected by the proposed method. The waveforms of direct current I_d, current valve No. 2 I_2 and current valve No. 6 I_6, are shown in Figure 7.
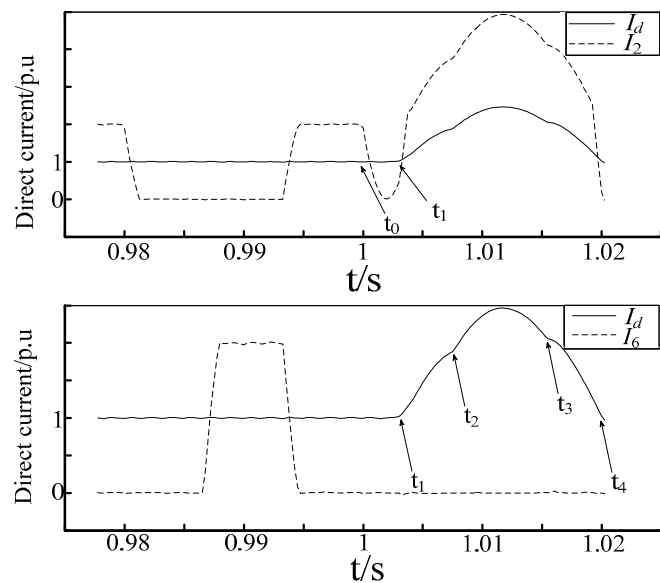
Figure 7. Direct current and Nos. 2 and 6 valve current in the C phase serious fault.

Slightly before t_1 = 1.003 s, valve No. 2 turn on again soon after the end of its conduction. The first CF occurred. Latter 2-5 valve bridge forms the DC short circuit, and the direct current has been greatly improved at t_1.

The second CF occurs at t_2 = 1.008 s. The reason for the singularity of current waveform at t_2 is that valve No. 6 does not turn on. The current continues to flow through the No. 2 valve, and then the 2-5 bridge forms another DC short circuit.

Compared with the three-phase symmetrical fault, the converter in the single-phase fault produces a large number of harmonics. The phase locked loop (PLL), which is based on the three-phase symmetry model and determines the firing order of each valve, is affected by the asymmetrical voltage and harmonics. In addition, the voltage zero-crossing points drifts [25], thus making part of the valve firing signals ahead or delay. Valve No. 6 is on the upper bridge of phase b. The firing signal must be received by the valve when the voltage of phase b is in its highest 1/6 cycles. The instability of PLL output affects this itinerary. This is the reason that CF occurs at t_2.

The 3rd and 4th CF occurs at t_3 and t_4, respectively. The reason is similar to those of t_1 and t_2.

According to the proposed method, the wavelet coefficients of current waveform are obtained and shown in Figure 8. The CF moment t_1 to t_4 is detected by their prominent wavelet coefficients. The detection results are illustrated in Table 2.
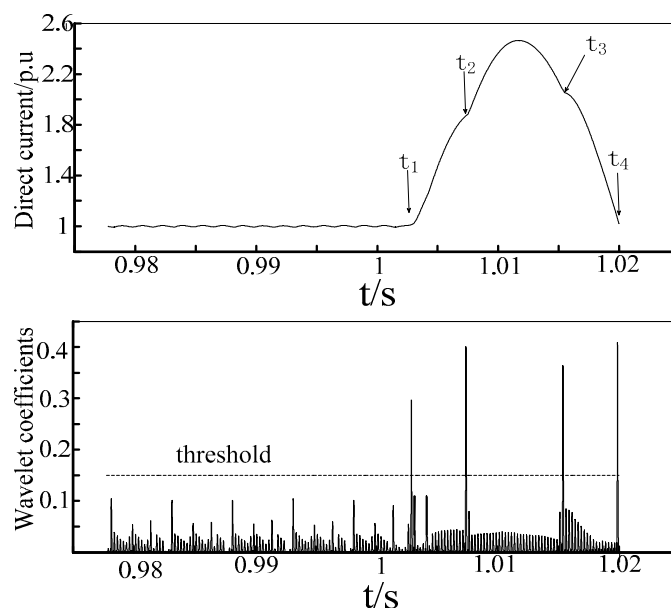
Figure 8. Direct current wavelet coefficients of C phase serious fault.

Table 2. Simulation and detection result of CF moments in C phase serious fault.

Comparasion	1st CF (t_1)	2nd CF (t_3)	3rd CF (t_3)	4th CF (t_4)	Controller Point
Simulation	1.003 s	1.014 s	1.016 s	1.019 s	1.011 s
Proposed method	1.003 s	1.014 s	1.016 s	1.019 s	Not detected

- (b) Detection results for slight single-phase fault

For the HVDC benchmark, set the fault as C phase grounding fault in the inverter with Zf = 100 Ω. In this case, the growth of direct current is only related to the voltage drop on the inverter side, and the wavelet coefficients of the corresponding direct current waveform are shown in Figure 9. The wavelet coefficients of each sample point do not exceed the threshold (0.15).
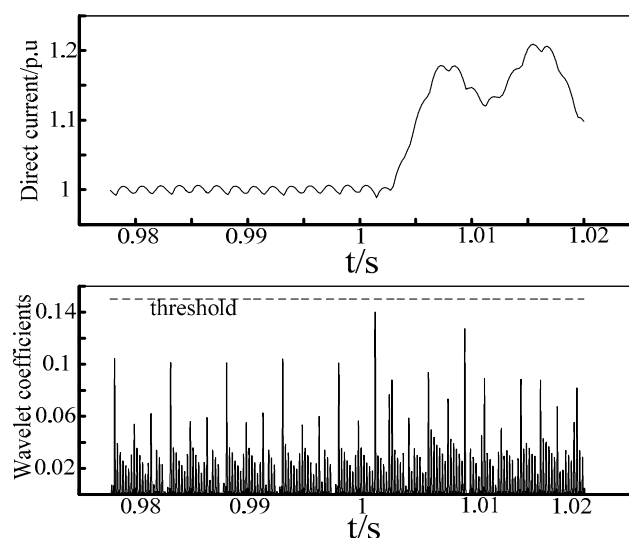

Figure 9. Direct current wavelet coefficients of C phase non-commutation failure.

- (c) Detection results for rectifier single-phase fault

Set the fault as C phase grounding fault in the rectifier with Zf = 10 Ω. In this case, the fault will not lead to CF. The corresponding direct current waveform wavelet coefficients are shown in Figure 10, none of which exceed the threshold (0.15).
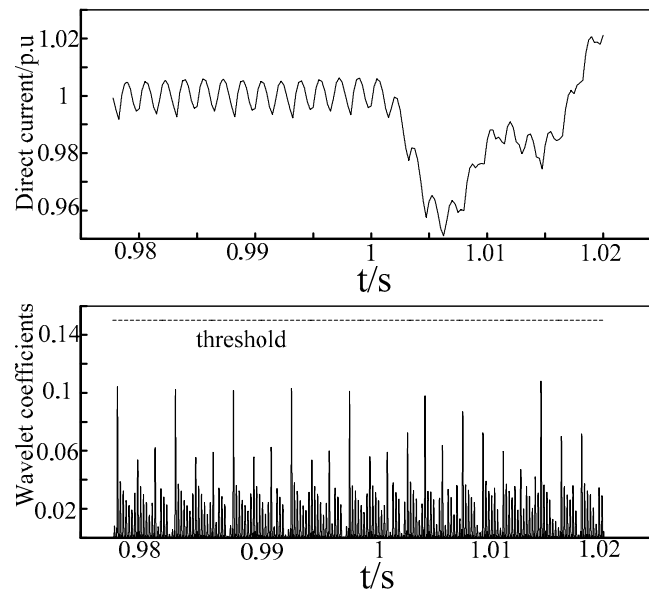

Figure 10. Direct current wavelet coefficients of C phase fault in rectifier.

Section 5.1.2 shows that the proposed detection method has a good relevance for CF. The wavelet coefficients of direct current can quickly indicate whether or not CF has occurred.

5.1.3. Two-Phase Fault Detection Results

For the HVDC benchmark, set the fault as B-C phase fault in the inverter with Zf = 10 Ω. The waveforms of direct current I_d, current valve No. 4 I_4 are shown in Figure 11.
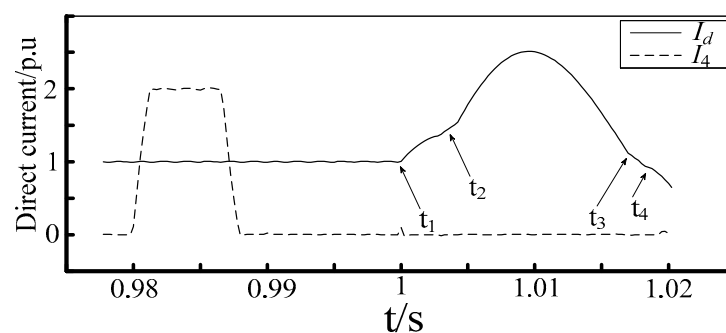

Figure 11. Direct current and No. 4 valve current in the B-C phase fault.

The first DC short circuit occurs at t_1 = 1.001 s, when conduction of valve No.4 lasts a short period of time. The direct current flow through the 2-3 bridge. As B-C phase short circuit exists, these two phase voltages are almost equal, and then 2 and 3 valve form an "abnormal" DC short circuit.

The second DC short circuit occurs at t_2 = 1.003 s, when valve No. 5 normally turns on. No. 2 and No. 5 valve conduct at the same time and form a "normal" short circuit. The reasons why CF occurs at t_3, t_4 are similar to those of t_1 and t_2.

The detection result of the B-C phase fault by the proposed method is shown in Figure 12. By comparing with the wavelet coefficient threshold, the method can accurately determine t_1 to t_4 moments. The detection results are illustrated in Table 3.
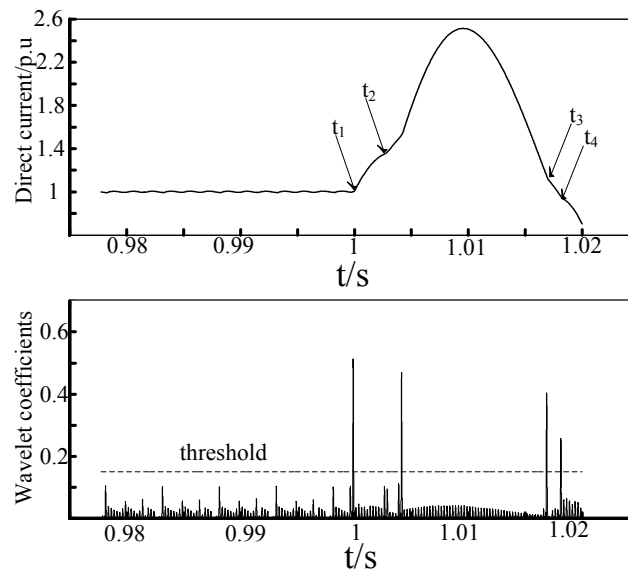
Figure 12. Direct current wavelet coefficients of B-C phase fault.

Table 3. Simulation and detection result of CF moments in B-C phase serious fault.

Comparasion	1st CF (t_1)	2nd CF (t_3)	3rd CF (t_3)	4th CF (t_4)	Controller Point
Simulation	1.001 s	1.003 s	1.018 s	1.019 s	1.009 s
Proposed method	1.001 s	1.003 s	1.018 s	1.019 s	Not detected
Gradient method	1.001 s	Not detected	Not detected	Not detected	1.007 s

Compared with the literature [27], this method is more accurate in judging the exact time of CF in the serious fault. Figure 13 shows the results of the DC waveform and the gradient calculation in the case of the inverter B-C phase fault, where transition resistance is 10 Ω, in Ref. [27].
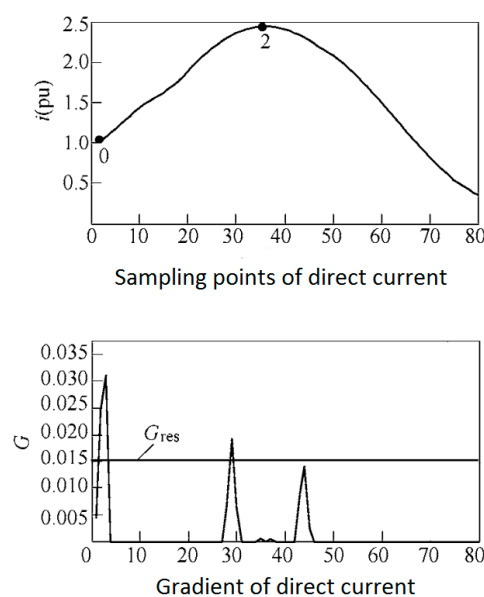
Figure 13. DC Waveform and Gradient in the B-C phase fault.

By the gradient method in Ref. [27], moment "0" and "2" can be detected for their prominent morphological gradient. However, moment "2" (1.007) is the controller point, which should not be detected.

The results of the same case by the proposed method are shown in Figure 12 and Table 3, and the two CF points (t_1, t_2) before the controller point can be accurately detected. At the same time, the wavelet coefficients at the controller point are not obvious. Comparison proves that the method is more accurate in the time domain and is more relevant for CF.

5.1.4. Discussion

- In above cases, it is considered that 0.15 is a reasonable threshold to determine whether CF occurs. A more appropriate valve should be selected according to the data length of wavelet and sampling frequency, so as to adapt to engineering practice.
- The increment of sampling frequency can promote the detection effectiveness of the proposed method. However, a too high sampling frequency will also lead to the problems such as the high cost of monitoring equipment and heavy burden on the communication system. The balance between cost and effectiveness should be considered.

To test the rationality of the above viewpoint on sampling frequency, the three-phase fault with Zf = 100 Ω, as is shown in Section 5.1.1, is selected to do further tests. In order to illustrate the impact of sampling frequency on the successful CF detection, two cases with sampling frequency of 2000 Hz and 1000 Hz with the same fault are studied. The results are shown in Figures 14 and 15.
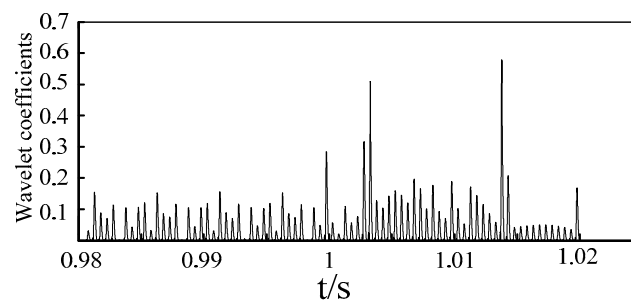

Figure 14. Direct current wavelet coefficients of three-phase grounding fault, Zf = 100 Ω, 2000 Hz.

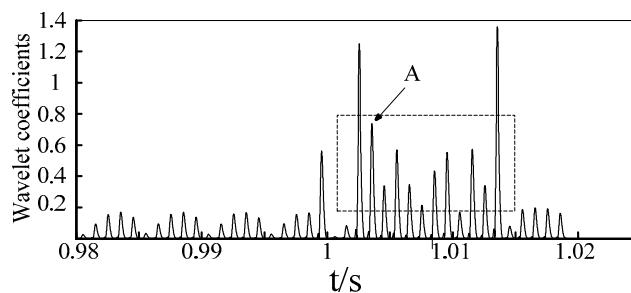**Figure 15.** Direct current wavelet coefficients of three-phase grounding fault, Zf = 100 Ω, 1000 Hz.

Comparing Figures 6, 14 and 15, the following conclusions can be summarized.

(1)   With the increase of sampling frequency, the values of wavelet coefficient decreased. Correspondingly, the threshold that judges CF occurrence should decrease as well.
(2)   More importantly, with the increase of sampling frequency, the difference of wavelet coefficient between CF point and non-communication failure point became clearer.

In Figure 15, the maximum wavelet coefficients of non-CF point in fault duration, as point A in the box, is 0.77. The wavelet coefficients of CF point is 1.27 and 1.37, nearly 1.5 times as that of the non-CF point. In Figure 6, the wavelet coefficients of non-communication failure point in fault duration are 0.06.The CF point is 0.48 and 0.34, nearly 6–8 times as that of the non-CF point.

In conclusion, a higher sampling rate will help identify CF points. However, a too high sampling frequency will also lead to the problems such as the high cost of monitoring equipment and heavy burden on the communication system. Considering the balance between cost and effectiveness, 4000 Hz is the selected sampling frequency in this paper.

5.2. Investigation of the Proposed Additional Emergency Control for CF

To evaluate the validity of proposed AECCF, the following two fault scenarios are illustrated:

1. Three-phase grounding fault with Zf = 100 Ω (same with Section 5.1.1),
2. C phase serious grounding fault with Zf = 70 Ω (same with Section 5.1.2 (a)).

The performances of the system with and without AECCF under the above scenarios are as shown in Figures 16 and 17.

From Figure 16, the following two conclusions can be summarized:

- The extinguishing angle rises at moment t_1 (1.015 s) by AECCF, earlier than that by normal controllers at t_2 (1.022 s). The duration of CF is shortened by AECCF.
- The curve of extinguishing angle by AECCF is below that of normal controllers from 1.06 s, which means that AECCF has a role in promoting the recovery of extinguishing angle.
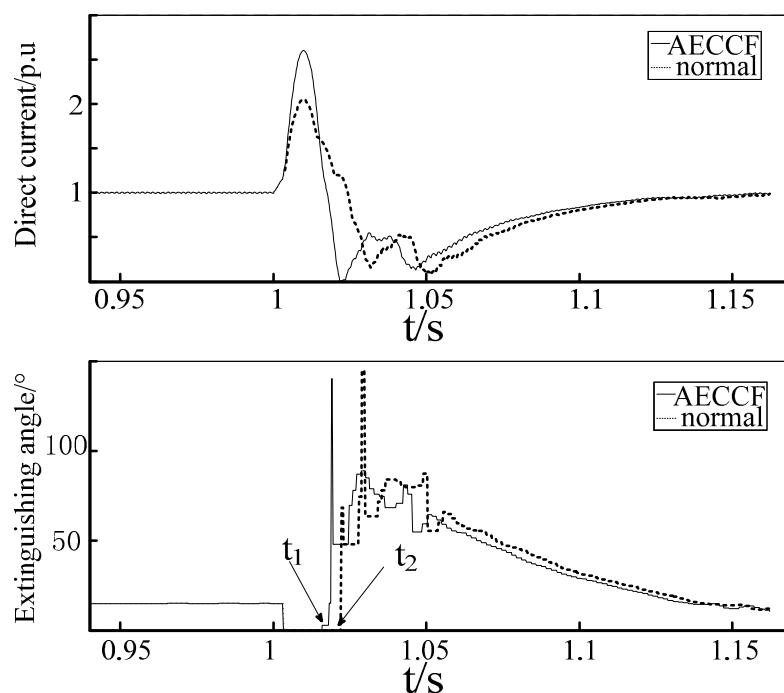

Figure 16. Extinguishing angle and direct current with normal controls and with additional emergency control for CF (AECCF) in three-phase grounding fault.
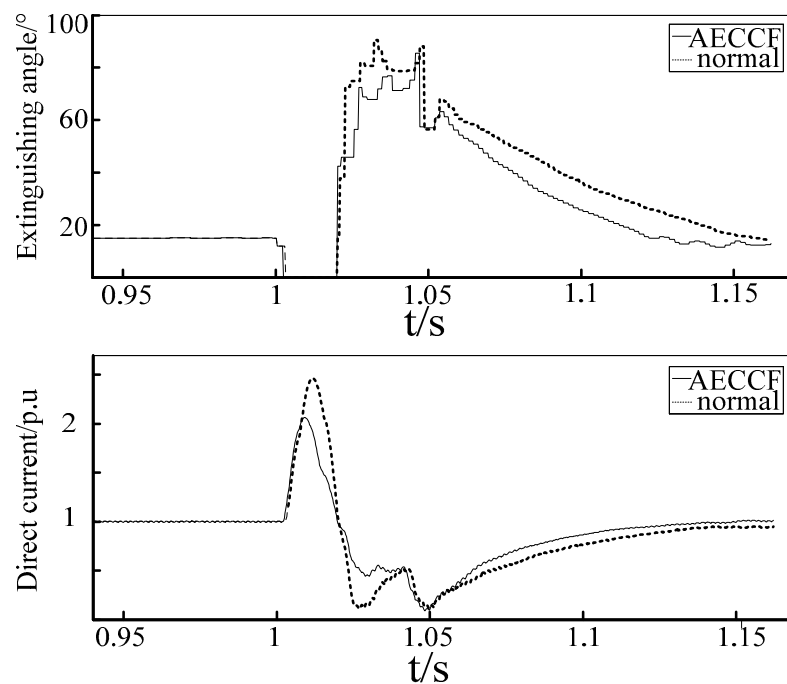
Figure 17. Extinguishing angle and direction current with normal controls and with AECCF in C phase serious fault.

In conclusion, based on the accuracy and sensitivity of the proposed detection method, the proposed AECCF can rapidly increase safety margin and prevent subsequent CFs. The recovery of extinguishing angle after fault can be improved as well.

6. Conclusions

In this paper, a novel detection method for consecutive CF via Daubechies wavelet with 2nd-order vanishing moments is proposed, based on the characteristic analyses of the waveforms of direct current in CF. Once the wavelet coefficients of the sampling points are detected to exceed the threshold, the occurrence of CF is confirmed. Furthermore, an additional emergency control for preventing subsequent CF is proposed. The proposed CF detection method is based on the direct current waveform, which is available for the converter station. The whole process of proposed CF detection method and AECCF are closely related. Therefore, the fast response of AECCF is guaranteed by the rapidity of the proposed CF detection method.

(1)   By analyzing the physical characteristics of the direct current waveform of the converter station in CF, the 2nd and higher order derivative values of the direct current are summarized as the core to judge CF.

(2)   On the basis of moment selection characteristics, the Daubechies wavelet coefficient, which can represent the 2nd and higher order derivative values of direct current, is established. Once the wavelet coefficients of the sampling points are detected to exceed the threshold, the occurrence of CF is confirmed. The proposed detection method of CF has good performances in regards to accuracy and sensitivity.

(3)   Furthermore, by instantly increasing advanced firing angle β in the inverter side, an additional emergency control strategy is proposed to increase safety margin and prevent subsequent CFs.

In this paper, Constant Current and Constant Extinguish Angle strategies, which are utilized in the benchmark model, are considered. The effect of some other control strategies, by whose function the direct current may have different singularity in CF, will be further investigated in the future.

Author Contributions: Ziyu Guo and Tao Lin conceived of the main idea and wrote the manuscript. Liyong Wang contributed the simulation environment. Rusi Chen and Ruyu Bi analyzed the data.

Conflicts of Interest: The authors declare no conflict of interest.

References

1. Arrillaga, J. *High Voltage Direct Current Transmission*, 2nd ed.; Institute of Electrical and Electronics Engineers Publications: Piscataway, NJ, USA, 1998.
2. Devarapalli, R.; Pandey, R. Analysis of weak AC system interface with multi-infeed HVDC. In Proceedings of the International Conference on Computing, Electronics and Electrical Technologies (ICCEET), Kumaracoil, India, 21–22 March 2012; pp. 138–144.
3. Lin, C.H. Effect of Commutation Failures on Torsional Vibrations of a Turbine Generator nearby an HVDC Link. *J. Mar. Sci. Technol.* **2010**, *18*, 69–76.
4. Sato, M.; Honjo, N.; Yamaji, K.; Yoshino, T.; Arai, J. HVDC converter control for fast power recovery after AC system fault. *IEEE Trans. Power Deliv.* **1997**, *12*, 1319–1326. [CrossRef]
5. Hansen, A.; Havemann, H. Decreasing the commutation failure frequency in HVDC transmission systems. *IEEE Trans. Power Deliv.* **2002**, *15*, 1022–1026. [CrossRef]
6. Zhou, J.; Liu, C.; Zhao, J. Simulation analysis of commutation failure in a multi-infeed HVDC system. In Proceedings of the China International Conference on Electricity Distribution (CICED), Xi'an, China, 10–13 August 2016.
7. Reeve, J.; Lane-Smith, S.P. Multi-infeed HVDC transient response and recovery strategies. *IEEE Trans. Power Deliv.* **1993**, *8*, 1995–2001. [CrossRef]
8. Tang, M.; Ma, L.L.; Zhang, B. Optimal placement of dynamic reactive power compensation devices for improving immunity to commutation failure in multi-infeed HVDC systems. In Proceedings of the 4th International Conference on Systems and Informatics (ICSAI), Hangzhou, China, 11–13 November 2017.
9. Xue, Y.; Zhang, X.P.; Yang, C. Elimination of Commutation Failures of LCC HVDC System with Controllable Capacitors. *IEEE Trans. Power Syst.* **2016**, *31*, 3289–3299. [CrossRef]
10. Wei, Z.; Yuan, Y.; Lei, X.; Wang, H.; Sun, G.; Sun, Y. Direct-Current Predictive Control Strategy for Inhibiting Commutation Failure in HVDC Converter. *IEEE Trans. Power Syst.* **2014**, *29*, 2409–2417. [CrossRef]
11. Zhu, T.; Ning, W.; Ou, K. Discussion on commutation failure in HVDC transmission system. *Power Syst. Prot. Control* **2008**, *36*, 116–120.
12. Zhu, T.; Wang, C. Analysis and recovery of commutation failure in Tian-Guang HVDC transmission system. *High Volt. Eng.* **2008**, *34*, 1769–1773.
13. Rahimi, E.; Gole, A.M.; Davies, J.B.; Fernando, I.T.; Kent, K.L. Commutation failure in single- and multi-infeed HVDC systems. In Proceedings of the 8th IEE International Conference on AC and DC Power Transmission, London, UK, 28–31 March 2006; pp. 182–186.
14. Thio, C.V.; Davies, J.B.; Kent, K.L. Commutation failures in HVDC transmission systems. *IEEE Trans. Power Deliv.* **1996**, *11*, 946–957. [CrossRef]
15. Liu, X.; Wang, Z.; Yang, Y.; Li, L. A concurrent commutation failure detection method for multi-infeed HVDC systems. In Proceedings of the IEEE 18th Workshop on Control and Modeling for Power Electronics (COMPEL), Stanford, CA, USA, 9–12 July 2017; pp. 1–5.
16. Shao, Y.; Tang, Y. Fast Evaluation of Commutation Failure Risk in Multi-infeed HVDC Systems. *IEEE Trans. Power Syst.* **2018**, *33*, 646–653. [CrossRef]
17. Liao, Z.; Luo, L. Research on fault diagnosis of HVDC commutation failure. In Proceedings of the IEEE International Conference on High Voltage Engineering and Application (ICHVE), Chengdu, China, 19–22 September 2016; pp. 1–4.
18. Rahimi, E.; Gole, A.M.; Davies, B.; Fernando, I.; Kent, K. Commutation failure analysis in multi-infeed HVDC systems. *IEEE Trans. Power Deliv.* **2011**, *26*, 378–384. [CrossRef]

19. Liang, Y.; Lin, X.; Gole, A.M.; Yu, M. Improved Coherency-Based Wide-Band Equivalents for Real-Time Digital Simulators. *IEEE Trans. Power Syst.* **2011**, *26*, 1410–1417. [CrossRef]

20. Guo, C.; Liu, Y.; Zhao, C.; Wei, X.; Xu, W. Power Component Fault Detection Method and Improved Current Order Limiter Control for Commutation Failure Mitigation in HVDC. *IEEE Trans. Power Deliv.* **2015**, *30*, 1585–1593. [CrossRef]

21. Chen, S.Y.; Li, X.N.; Yu, J. Method based on the sin-cos components detection mitigates commutation failure in HVDC. *Proc. CSEE* **2005**, *25*, 1–6.

22. Lv, P.; Wang, M.; Xu, H. Analysis of commutation failure reason in three Gorges Guangdong HVDC system Echeng station. *Relay* **2005**, *33*, 75–78.

23. Zhang, L.; Dofnas, L. A novel method to mitigate commutation failures in HVDC systems. In Proceedings of the International Conference on Power System Technology, Kunming, China, 13–17 October 2002; pp. 51–56.

24. Sun, Y.Z.; Peng, L.; Ma, F.; Li, G.J.; Lv, P.F. Design a Fuzzy Controller to Minimize the Effect of HVDC Commutation Failure on Power System. *IEEE Trans. Power Syst.* **2008**, *23*, 100–107. [CrossRef]

25. Zhong, Q.; Zhang, Y.; Lin, L. Diagnosis of commutation failure in HVDC systems based on wavelet transforms. In Proceedings of the Third International Conference on Electric Utility Deregulation and Restructuring and Power Technologies, Nanjing, China, 6–9 April 2008; pp. 1712–1717.

26. Gao, C.; Liao, Z.; Huang, S. Fault Diagnosis of Commutation Failures in the HVDC System Based on Wavelet Singular Value and Support Vector Machine. In Proceedings of the Asia-Pacific Power and Energy Engineering Conference, Wuhan, China, 27–31 March 2009; pp. 1–4.

27. Shen, H.; Huang, S.; Fei, B.; Li, O. A New Method to Detect Commutation Failure Based on Mathematical Morphology. *Trans. China Electrotech. Soc.* **2016**, *31*, 170–177.

28. Faruque, M.O.; Zhang, Y.; Dinavahi, V. Detailed modeling of CIGRE HVDC benchimark system using PSB/SIMULINK. *IEEE Trans. Power Deliv.* **2006**, *21*, 378–387. [CrossRef]

29. Daubechies, I. *Ten Lectures on Wavelets*; SIAM: Bangkok, Thailand, 1992.

30. Boggess, A.; Narcowich, F.J. *A First Course in Wavelets with Fourier Analysis*; Publishing House of Electronics Industry: Pearson, GA, USA, 2002.